Archive of Applied Mechanics 73 (2003) 481 – 494 © Springer-Verlag 2003
DOI 10.1007/s00419-003-0298-1

Effect of elastic wall motion on oscillatory flow of micropolar fluid in an annular tube

P. Muthu, B. V. Rathish Kumar, Peeyush Chandra

Summary Oscillatory flow of a micropolar fluid in an annular tube is investigated. The outer wall of the tube is taken to be elastic and the variation in the diameter of the elastic wall due to pulsatile nature of pressure gradient is assumed to be small. The wall motion is governed by a tube law. The nonlinear equations governing the fluid flow and the tube law are solved using perturbation analysis. The steady-streaming phenomenon due to the interaction of convected inertia with viscous effects is studied. The analysis, is carried out for zero mean flow rate. It presents the effects of the elastic nature of the wall combined with micropolar fluid parameters on the mean pressure gradient and wall shear stress for different catheter sizes and frequency parameters. It is found that the effect of micropolarity is of considerable importance for small steady-streaming Reynolds number. Also, it is observed that the relationship between mean pressure gradient and the flow rate depends on the amplitude of the diameter variation, flow rate waveforms and the phase difference between them.

Keywords: Oscillatory flow, Annular tube, Steady-streaming, Oscillatory pressure gradient, Micropolar fluid

1 Introduction

In clinical procedures, catheters are widely used for the purpose of measuring arterial pressure. The insertion of a catheter would modify the pressure distribution, hence, the pressure recorded by the transducer would differ from that in uncatheterized artery, however small the size of the catheter may be. Accordingly, the effect of the presence of catheter in the physiological arterial flows needs to be studied. Various experimental and analytical studies have been reported in the literature with respect to blood flow in catheterized artery. Paper [1] studied the extent to which a catheter insertion in the canine aorta influences the pressure which it records. An analysis of pulsatile blood flow in an annular region was presented in [2] to study the magnitude of error involved in the measurement of pressure distribution using catheter. Paper [3] estimated the increase of the mean flow resistance during coronary artery catheterization. In the above analytical studies, arterial wall was taken to be rigid. However, blood vessels are elastic in nature. It is observed that due to pulsatile blood pressure the artery diameter changes nearly 5–10%, and so artery can be treated as a thin-walled elastic tube see [4] where the nonlinear flow of a newtonian fluid was analysed in an elastic tube subjected to an oscillatory pressure gradient. The steady streaming phenomenon was discussed which is a characteristic of secondary flow due to wall motion and hence nonlinear convective acceleration. The results were applied to blood flow in an artery. By restricting the analysis to for zero mean-flow rate the authors of [4] indicated that the steady-streaming effect depends on the amplitude of the diameter variation, flow rate waveforms and the phase difference between them, which is an indicator of the influence of wave reflection. Subsequently the analysis was extended to nonzero mean flow rate also, [5].

In a recent analysis, paper [6] considered a mathematical model to study the combined effect of the introduction of a catheter and elastic properties of the arterial wall on the pulsatile nature

Received 11 June 2002; accepted for publication 15 May 2003

P. Muthu, B. V. Rathish Kumar, Peeyush Chandra (✉)
Department of Mathematics, Indian Institute of Technology,
Kanpur - 208 016, India
e-mail: peeyush@iitk.ac.in
Fax: +91-512-2597500

of blood flow. The authors provided a relationship between mean pressure gradient and the flow rate assuming zero mean flow rate and the newtonian fluid model for blood. It is well known that blood is a suspension of red and white blood cells and other smaller constituents in electrolytic aqueous solution of plasma. It imparts thus a non-newtonian behaviour to the rheology of blood. Various models have been suggested to account for such behaviour of blood. In particular, micropolar fluid theory, [7], [8], has been applied to physiological fluids, including blood, to account for the suspension nature of the fluid [9]. The micropolar fluid model characterizes suspension of neutrally buoyant rigid spherical particles in a viscous fluid, where the individuality of substructures affects the flow. Basically, these fluids support couple stresses and body couples and exhibit microrotational effects. Analyses presented in [8] and [10] compared theoretical velocity profiles for blood flow, using micropolar fluid model, with the experimentally determined profiles, both in steady and pulsatile cases. The comparison was found to be in good agreement.

In view of this, an attempt has been made to assess the magnitude of mean pressure gradient and mean wall shear stress in the flow of micropolar fluid in an annular tubular region with elastic outer wall. The equations of the fluid motion supplemented by the response of the wall are solved by perturbation technique, assuming small wall-diameter variation. The analysis is carried out for zero mean flow rate and is restricted to small steady-streaming Reynolds number.

2
Formulation of the problem

We consider a fully developed unsteady flow of an incompressible micropolar fluid in the annular region between the catheter and the flexible elastic wall. The geometry is shown in Fig. 1 with respect to the cylindrical coordinate system (R, Θ, Z). The outer boundary is taken as an isotropic, thin-walled elastic circular cylindrical tube moving in the radial direction at negligible axial deformation. Let R_0 be the mean radius of the elastic tube, which corresponds to the original undisturbed tube. The catheter is modelled by a co-axial tube with radius kR_0, $k < 1$.

Following [4], the elastic nature of the boundary wall movement under excessive internal fluid pressure $(P - P_o)$ can be described by the following tube law (pressure-radius relationship):

$$\frac{R_s(P)}{R_0} = 1 + \frac{1}{2}\bar{D}(P - P_0) + \cdots \quad . \tag{1}$$

Here, $R = R_s(Z, \tau)$ is the instantaneous radius of the tube at the instant τ, P is the pressure, P_0 the mean pressure and $\bar{D}$ is the distensibility of the tube wall.

As we consider here the flow to be oscillatory, this will have an influence, however small, on the instantaneous position of the flexible catheter. Though there may be very little movement away from the center of the artery, there would be axial movement of the catheter. In other words, the wave propagating in the fluid is transmitted to the catheter as well. It is considered that the axisymmetric motion of the catheter is periodic along the Z axis and it is in phase lead

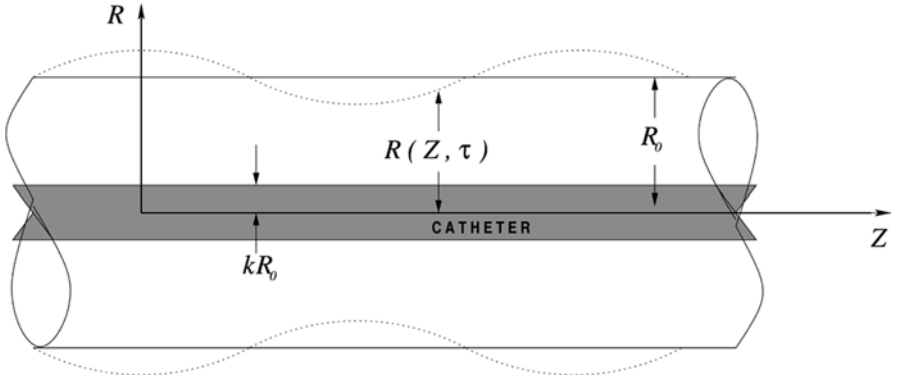

Fig. 1. Geometry of a catheterized artery with wall movement

over the flow rate with small constant amplitude. This leads to the boundary conditions for velocity components U and W (in R and Z directions, respectively) as

$$U = 0, \quad W = W_c(\tau) \qquad \text{at } R = kR_0 \ , \tag{2}$$

where $W_c(\tau)$ describes the movement of the flexible catheter influenced by the oscillatory nature of flow, with frequency ω. The boundary conditions on the wall are prescribed by the no-slip condition as

$$U = \frac{\partial R_s}{\partial \tau}, \quad W = 0 \qquad \text{at } R = R_s(Z,\tau) \ . \tag{3}$$

Further, it is assumed that due to the fluid-solid interaction at both boundaries, the microstructure does not rotate relative to the catheter surface as well as relative to the elastic boundary, [11] which gives

$$G = 0 \quad \text{at } R = kR_0 \ \text{at } R = R_s(Z,\tau) \ , \tag{4}$$

where G is the nonvanishing component of the microrotational velocity vector $(0, G(R,Z,\tau), 0)$. Now, for the axisymmetric flow of a micropolar fluid, the governing equations using cylindrical coordinates can be written in nondimensional form as follows:

$$\frac{\partial u}{\partial r} + \frac{\partial w}{\partial z} + \frac{u}{r} = 0 \ , \tag{5}$$

$$S_t^2\left(\frac{\partial u}{\partial t} + u\frac{\partial u}{\partial r} + w\frac{\partial u}{\partial z}\right) = -\frac{\partial p}{\partial r} + \frac{S_t^2(2+\mu_1)}{2\alpha^2}\left(\frac{\partial^2 u}{\partial r^2} + \frac{1}{r}\frac{\partial r}{\partial r} - \frac{u}{r^2} + S_t^2\frac{\partial^2 u}{\partial z^2}\right) - \frac{S_t^2\mu_1}{\alpha^2}\frac{\partial g}{\partial z} \ , \tag{6}$$

$$\frac{\partial w}{\partial t} + u\frac{\partial w}{\partial r} + w\frac{\partial w}{\partial z} = -\frac{\partial p}{\partial z} + \frac{(2+\mu_1)}{2\alpha^2}\left(\frac{\partial^2 w}{\partial r^2} + \frac{1}{r}\frac{\partial w}{\partial r} + S_t^2\frac{\partial^2 w}{\partial z^2}\right) + \frac{\mu_1}{\alpha^2}\left(\frac{\partial g}{\partial r} + \frac{g}{r}\right) \ , \tag{7}$$

$$j\alpha^2 M\left(\frac{\partial g}{\partial t} + u\frac{\partial g}{\partial r} + w\frac{\partial g}{\partial z}\right) = \left(\frac{\partial^2 g}{\partial r^2} + \frac{1}{r}\frac{\partial g}{\partial r} - \frac{g}{r^2}\right) + {S_t}^2\frac{\partial^2 g}{\partial z^2} + \mu_1 M\left({S_t}^2\frac{\partial u}{\partial z} - \frac{\partial w}{\partial r} - 2g\right) \ , \tag{8}$$

under the nondimensional scheme as given below:

$$r = \frac{R}{R_0}, \quad z = \frac{\omega Z}{C_0}, \quad t = \tau\omega, \quad p = \frac{P - P_0}{\rho C_0^2}, \quad u = \frac{U}{R_0\omega}, \quad w = \frac{W}{C_0}, \quad \tilde{w} = \frac{W_c}{C_0},$$

$$g = \frac{G}{C_0/R_0}, j = \frac{J}{R_0^2}, \quad \mu_1 = \frac{\kappa}{\mu}, \quad M = \frac{R_o^2\mu}{\gamma}, \quad N = \left(\frac{\mu_1}{2+\mu_1}\right)^{\frac{1}{2}}, \quad \epsilon = \frac{R_{\max} - R_0}{R_0},$$

$$\alpha = R_0\left(\frac{\omega\rho}{\mu}\right)^{\frac{1}{2}}, \quad S_t = \frac{\omega R_0}{C_0}, \quad r_s(z,t) = \frac{R_s(Z,\tau)}{R_0}, \quad C_0 = \frac{1}{(\rho\bar{D})}^{\frac{1}{2}} \ ,$$

where ρ is the density of the fluid; J is the microinertia constant; μ, κ and γ are the viscosity coefficients of micropolar fluids, called dynamic viscosity, vortex viscosity and material constant, respectively; $R_{\max}$ is the maximum radius attained by the tube wall due to the oscillatory pressure on the elastic wall of the tube and C_0 is the wave speed.

In the above equations, α is the Womersley parameter, parameters μ_1 and M are nondimensional quantities due to micropolar fluid flow, μ_1 denotes the ratio of the viscosity coefficient corresponding to micropolar fluids to the classical viscosity coefficient, M depends upon the size of the microstructure. It can be noted that when κ and γ are zero, that is, when μ_1 becomes zero and M tends to infinity, Eqs. (5) to (8) reduce to the one which describes the behaviour of the classical newtonian fluid flow. Remember j is the nondimensional form of the microinertia constant J.

The boundary conditions become

$$g = 0, \quad u = 0 \quad \text{and} \quad w = \tilde{w} \ \text{at} \ r = k \ , \tag{9}$$

$$g = 0, \quad u = \frac{\partial r_s}{\partial t} \quad \text{and} \quad w = 0 \ \text{at} \ r = r_s(z,t) \tag{10}$$

and the tube law is given by

$$r_s = 1 + \frac{1}{2}p + O(p^2) + \cdots \ . \tag{11}$$

Hereafter, we restrict ourselves to the case where $S_t = \omega R_0 / C_0$ is small, which amounts to considering the long-wavelength approximation. In view of this, the terms involving S_t^2 are neglected in the following analysis. Also, following Refs. [12] and [13], it is reasonable to assume that the nondimensional microinertia parameter is small $j \ll 1$, and accordingly we neglect this term in Eq. (8). Thus, the nondimensional governing equations reduce to

$$\frac{\partial u}{\partial r} + \frac{\partial w}{\partial z} + \frac{u}{r} = 0 \ , \tag{12}$$

$$\frac{\partial p}{\partial r} = 0 \ , \tag{13}$$

$$\frac{\partial w}{\partial t} + u\frac{\partial w}{\partial r} + w\frac{\partial w}{\partial z} = -\frac{\partial p}{\partial z} + \frac{(2+\mu_1)}{2\alpha^2}\left(\frac{\partial^2 w}{\partial r^2} + \frac{1}{r}\frac{\partial w}{\partial r}\right) + \frac{\mu_1}{\alpha^2}\left(\frac{\partial g}{\partial r} + \frac{g}{r}\right) \ , \tag{14}$$

$$\frac{\partial^2 g}{\partial r^2} + \frac{1}{r}\frac{\partial g}{\partial r} - \frac{g}{r^2} - \mu_1 M\left(\frac{\partial w}{\partial r} + 2g\right) = 0 \ , \tag{15}$$

with the boundary conditions as mentioned before.

To transform the problem of moving boundary to an immovable domain, we apply an affine transformation

$$\xi = 1 + (1-k)\left[\frac{r - r_s(p)}{r_s(p) - k}\right], \quad \text{where } 0 < k < 1 \ .$$

Thus, Eqs. (12)–(15) reduce to the following:

$$\frac{(1-k)}{(r_s-k)}\frac{\partial u}{\partial \xi} + \frac{(1-k)}{\xi_1}u + \frac{\partial w}{\partial z} - \frac{(\xi-k)}{(r_s-k)}\frac{\partial r_s}{\partial z}\frac{\partial w}{\partial \xi} = 0 \ , \tag{16}$$

$$\frac{\partial p}{\partial \xi} = 0 \ , \tag{17}$$

$$\begin{aligned}\frac{\partial w}{\partial t} = &-\frac{\partial p}{\partial z} + \frac{(2+\mu_1)}{2\alpha^2}\left(\frac{1-k}{r_s-k}\right)^2\left[\frac{\partial^2 w}{\partial \xi^2} + \frac{r_s-k}{\xi_1}\frac{\partial w}{\partial \xi}\right] - w\left[\frac{\partial w}{\partial z} - \frac{\xi-k}{r_s-k}\frac{\partial w}{\partial \xi}\frac{\partial r_s}{\partial z}\right] \\ &+ \left[(\xi-k)\frac{\partial r_s}{\partial t} - u(1-k)\right]\frac{1}{(r_s-k)}\frac{\partial w}{\partial \xi} + \frac{\mu_1}{\alpha^2}\left[\left(\frac{1-k}{r_s-k}\right)\frac{\partial g}{\partial \xi} + \frac{(1-k)}{\xi_1}g\right] \ ,\end{aligned} \tag{18}$$

$$\left(\frac{1-k}{r_s-k}\right)^2\left[\frac{\partial^2 g}{\partial \xi^2} + \frac{(r_s-k)}{\xi_1}\frac{\partial g}{\partial \xi} - \left(\frac{r_s-k}{\xi_1}\right)^2 g\right] - \mu_1 M\left[\left(\frac{1-k}{r_s-k}\right)\frac{\partial w}{\partial \xi} + 2g\right] = 0 \ , \tag{19}$$

where $\xi_1 = (r_s - k)(\xi - 1) + r_s(1-k)$. The corresponding boundary conditions are

$$g = 0, \quad u = 0 \quad \text{and} \quad w = \tilde{w} \qquad \text{at} \ \xi = k \ , \tag{20}$$

$$g = 0, \quad u = \frac{\partial r_s}{\partial t} \quad \text{and} \quad w = 0 \qquad \text{at} \ \xi = 1 \ . \tag{21}$$

We take $\tilde{w} = w_c \cos(t - t_0)$, where $w_c \ll 1$ is the maximum amplitude of the catheter movement and t_0 is the phase lead of this motion over the flow. In general, w_c will depend on the elastic properties of the catheter material as well as on the tangential stress exerted by the fluid flow. However, here we treat w_c as a constant.

3 Analysis

The governing equations are coupled and nonlinear in nature and are not amenable to an analytic solution. Thus, we attempt for an approximate analytic solution using regular perturbation method with perturbation parameter ϵ, denoting the diameter variation parameter of the elastic wall due to pulsatile flow, which is small. It amounts to solving the problem for a slowly varying cross section of the annular region. Now, to solve Eqs. (16)–(21) for the flow field we assume

$$p = \epsilon p_{11} + \epsilon^2 (p_{20} + p_{21} + p_{22}) + O(\epsilon^3) \ , \tag{22}$$

$$r_s = 1 + \epsilon r_{s11} + \epsilon^2 (r_{s20} + r_{s21} + r_{s22}) + O(\epsilon^3) \ , \tag{23}$$

where p_{ij} represents the j^{th} harmonic (in terms of t) of the i^{th} order term in the expansion of p, and r_{sij} is defined analogously. The flow variables u, w and g are also assumed in a similar manner.

It may be remarked that the above perturbation forms in Eqs. (22)–(23) are sought on the basis of zero mean-flow rate. It means that flow rate as the input to the annulus is purely sinusoidal and the flow rate does not contain any steady component at $z = 0$ in the $O(\epsilon)$ case. Solution for the second-order case contains nonlinear interactions and will have both steady and oscillatory components.

The steady-streaming Reynolds number for micropolar fluid flow is defined as

$$R_{st} = \epsilon^2 \bar{\alpha}^2, \quad \text{where } \bar{\alpha}^2 = \frac{2\alpha^2}{2 + \mu_1} \ .$$

Further, as $\epsilon \ll 1$, it allows to take moderate values of R_{st} of order one for appropriate values of α. Thus, applying the arguments of Ref. [4] to the micropolar fluid flow, it may be noted that only the steady components, that is u_{20}, w_{20} and g_{20} alone contribute to the steady streaming up to $O(\epsilon^2)$. Therefore, while solving equations up to $O(\epsilon^2)$, we shall determine u_{20}, w_{20} and g_{20} only. Thus, our solutions are valid for small values of R_{st} and arbitrary values of α.

Substituting the perturbed form of the flow variables in Eqs. (16)–(21) and in the tube law, and collecting coefficients of similar powers of ϵ on both sides of the equations, we obtain the following sets of the governing equations and boundary conditions for u_{11}, w_{11}, g_{11}, u_{20}, w_{20}, g_{20}:

(1) equations corresponding to the case $O(\epsilon)$

$$\frac{\partial u_{11}}{\partial \xi} + \frac{u_{11}}{\xi} + \frac{\partial w_{11}}{\partial z} = 0 \ , \tag{24}$$

$$\frac{\partial p_{11}}{\partial \xi} = 0 \ , \tag{25}$$

$$\frac{\partial w_{11}}{\partial t} = -\frac{\partial p_{11}}{\partial z} + \frac{(2 + \mu_1)}{2\alpha^2} \left(\frac{\partial^2 w_{11}}{\partial \xi^2} + \frac{1}{\xi} \frac{\partial w_{11}}{\partial \xi} \right) + \frac{\mu_1}{\alpha^2} \left(\frac{\partial g_{11}}{\partial \xi} + \frac{g_{11}}{\xi} \right) \ , \tag{26}$$

$$\frac{\partial^2 g_{11}}{\partial \xi^2} + \frac{1}{\xi} \frac{\partial g_{11}}{\partial \xi} - \frac{g_{11}}{\xi^2} - \mu_1 M \left(\frac{\partial w_{11}}{\partial \xi} + 2 g_{11} \right) = 0 \ , \tag{27}$$

with boundary conditions yielding

$$g_{11} = 0, \quad u_{11} = 0 \quad \text{and} \quad w_{11} = \tilde{w} \qquad \text{at } \xi = k \ , \tag{28}$$

$$g_{11} = 0, \quad u_{11} = \frac{\partial r_{s11}}{\partial t} \quad \text{and} \quad w_{11} = 0 \qquad \text{at } \xi = 1 \ , \tag{29}$$

and the tube law gives

$$\frac{\partial r_{s11}}{\partial z} = \frac{1}{2}\frac{\partial p_{11}}{\partial z} \quad . \tag{30}$$

(2) equations corresponding to the case $O(\epsilon^2)$

$$\frac{\partial u_{20}}{\partial \xi} + \frac{u_{20}}{\xi} + \frac{\partial w_{20}}{\partial z} = G_2^*(\xi, z) \quad , \tag{31}$$

$$\frac{\partial p_{20}}{\partial \xi} = 0 \quad , \tag{32}$$

$$\frac{(2+\mu_1)}{2\alpha^2}\left(\frac{\partial^2 w_{20}}{\partial \xi^2} + \frac{1}{\xi}\frac{\partial w_{20}}{\partial \xi}\right) + \frac{\mu_1}{\alpha^2}\left(\frac{\partial g_{20}}{\partial \xi} + \frac{g_{20}}{\xi}\right) = \frac{\partial p_{20}}{\partial z} + G_1^*(\xi, z) \quad , \tag{33}$$

$$\frac{\partial^2 g_{20}}{\partial \xi^2} + \frac{1}{\xi}\frac{\partial g_{20}}{\partial \xi} - \frac{g_{20}}{\xi^2} - \mu_1 M\left(\frac{\partial w_{20}}{\partial \xi} + 2g_{20}\right) = G_3^*(\xi, z) \quad , \tag{34}$$

where

$$G_1(\xi, z, t) = w_{11}\frac{\partial w_{11}}{\partial z} - \left(\xi_2 \frac{\partial r_{s11}}{\partial t} - u_{11}\right)\frac{\partial w_{11}}{\partial \xi} + \frac{\mu_1}{\alpha^2}\left(\frac{1}{1-k}\frac{\partial g_{11}}{\partial \xi} + \frac{\xi_2}{\xi^2} g_{11}\right) + \frac{r_{s11}(2+\mu_1)}{2\alpha^2}\left[\frac{2}{1-k}\frac{\partial^2 w_{11}}{\partial \xi^2} + \frac{2\xi - k}{\xi^2(1-k)}\frac{\partial w_{11}}{\partial \xi}\right] \quad ,$$

$$G_2(\xi, z, t) = \xi_2 \frac{\partial r_{s11}}{\partial z}\frac{\partial w_{11}}{\partial \xi} - \frac{r_{s11}}{1-k}\frac{\partial w_{11}}{\partial z} - \frac{k r_{s11}}{\xi^2(1-k)} u_{11} \quad ,$$

$$G_3(\xi, z, t) = r_{s11}\left[\frac{2}{1-k}\frac{\partial^2 g_{11}}{\partial \xi^2} + \frac{2\xi - k}{\xi^2(1-k)}\frac{\partial g_{11}}{\partial \xi} - \frac{2\,\xi_2}{\xi^3} g_{11}\right] - \mu_1 M\left(\frac{r_{s11}}{1-k}\frac{\partial w_{11}}{\partial \xi}\right) \quad .$$

with boundary conditions

$$g_{20} = 0, \quad u_{20} = 0 \quad \text{and} \quad w_{20} = 0 \qquad \text{at } \xi = k \quad , \tag{35}$$

$$g_{20} = 0, \quad u_{20} = 0 \quad \text{and} \quad w_{20} = 0 \qquad \text{at } \xi = 1 \quad . \tag{36}$$

Here, the quantities G_1^*, G_2^* and G_3^* are time-averaged quantities of G_1, G_2 and G_3 respectively

$$\xi_2 = \frac{\xi - k}{1-k} \quad .$$

3.1
Solution for the $O(\epsilon)$ case

Since the fluid motion is oscillatory with frequency ω, we assume

$$\frac{\partial p_{11}}{\partial z} = \mathrm{Re}\{f(z)\mathrm{e}^{it}\} = \frac{1}{2}\left\{f(z)\mathrm{e}^{it} + \overline{f(z)}\mathrm{e}^{-it}\right\} \quad , \tag{37}$$

where f is an unknown function of z only, to be determined from the tube law and the axial boundary conditions; Re indicates the real part of a complex variable and the overline denotes complex conjugate. Similarly, for g_{11}, u_{11}, w_{11} and r_{s11} we assume the following forms:

$$g_{11} = \mathrm{Re}\{G_{11}(\xi, z)\mathrm{e}^{it}\}, \quad u_{11} = \mathrm{Re}\{U_{11}(\xi, z)\mathrm{e}^{it}\} \quad , \tag{38}$$

$$w_{11} = \mathrm{Re}\{W_{11}(\xi, z)\mathrm{e}^{it}\} \quad \text{and} \quad r_{s11} = \mathrm{Re}\{B(z)\mathrm{e}^{it}\} \quad . \tag{39}$$

On substituting these forms in Eqs. (24) to (29), we get the expressions for G_{11} and W_{11} in the following form:

$$G_{11}(\xi,z) = c_1(z)I_1(\alpha_{11}\xi) + c_2(z)K_1(\alpha_{11}\xi) + d_1(z)I_1(\alpha_{12}\xi) + d_2(z)K_1(\alpha_{12}\xi) \ , \tag{40}$$

$$W_{11}(\xi,z) = \tilde{a}_{11}[c_1(z)I_0(\alpha_{11}\xi) - c_2(z)K_0(\alpha_{11}\xi)] + \tilde{a}_{12}[d_1(z)I_0(\alpha_{12}\xi) - d_2(z)K_0(\alpha_{12}\xi)] + if(z) \tag{41}$$

where I_0, I_1 and K_0, K_1 denote Bessel functions, and

$$\alpha_{11}^2 = \frac{z_1 - \sqrt{z_1^2 - 4z_2}}{2}, \quad \alpha_{12}^2 = \frac{z_1 + \sqrt{z_1^2 - 4z_2}}{2} \ ,$$

$$z_1 = \alpha_1^2 + a^2(1 - N^2), \quad z_2 = \alpha_1^2 a^2, \quad a^2 = 2\mu_1 M, \quad \alpha_1 = \sqrt{i\bar{\alpha}^2} \ .$$

Here, $a_{11}, a_{12}, \tilde{a}_{11}, \tilde{a}_{12}$ are known constants and $c_1(z)$, $c_2(z)$, $d_1(z)$ and $d_2(z)$ are unknown functions, to be determined by the linear system of equations, which is obtained on using the boundary conditions Eqs. (28) and (29). Using the equation of continuity (24) and boundary condition (28) for u_{11}, we get U_{11} as

$$\begin{aligned} U_{11}(\xi,z) = -\Bigg\{ & \frac{\tilde{a}_{11}}{\alpha_{11}} \left[c_1^{(1)}(z)\left(I_1(\alpha_{11}\xi) - \frac{k}{\xi} I_1(\alpha_{11}k) \right) + c_2^{(1)}(z)\left(K_1(\alpha_{11}\xi) - \frac{k}{\xi} K_1(\alpha_{11}k) \right) \right] \\ & + \frac{\tilde{a}_{12}}{\alpha_{12}} \left[d_1^{(1)}(z)\left(I_1(\alpha_{12}\xi) - \frac{k}{\xi} I_1(\alpha_{12}k) \right) + d_2^{(1)}(z)\left(K_1(\alpha_{12}\xi) - \frac{k}{\xi} K_1(\alpha_{12}k) \right) \right] \Bigg\} \\ & - i\left(\frac{\xi}{2} - \frac{k^2}{2\xi} \right) f^{(1)}(z) \ , \end{aligned} \tag{42}$$

where the superscript within parenthesis indicates derivative with respect to z. The other boundary condition,

$$u_{11} = \frac{\partial r_{s11}}{\partial t} \quad \text{at } \xi = 1$$

gives the expression for the wall amplitude as

$$B(z) = -iU_{11}(1,z) \ .$$

Further using the tube law, Eq. (30), the unknown function f is determined as

$$f(z) = \left[A_{11} + \frac{-\int e^{-imz}\, s_1\, dz}{-2im} \right] e^{imz} + \left[A_{12} + \frac{\int e^{imz} s_1\, dz}{-2im} \right] e^{-imz} \ , \tag{43}$$

where

$$\begin{aligned} s_1(z) = 2m^2 i \Bigg\{ & \frac{\tilde{a}_{11}}{\alpha_{11}} \left[c_1^{(2)}(z)(I_1(\alpha_{11}) - kI_1(\alpha_{11}k)) + c_2^{(2)}(z)(K_1(\alpha_{11}) - kK_1(\alpha_{11}k)) \right] \\ & + \frac{\tilde{a}_{12}}{\alpha_{12}} \left[d_1^{(2)}(z)(I_1(\alpha_{12}) - kI_1(\alpha_{12}k)) + d_2^{(2)}(z)(K_1(\alpha_{12}) - kK_1(\alpha_{12}k)) \right] \Bigg\} \ , \end{aligned}$$

and

$$m^2 = \frac{1}{1 - k^2} \ ,$$

while A_{11} and A_{12} are constants to be determined.

The nondimensional flow rate q is given by

$$q = \int_k^1 \xi w_{11}(\xi, z, t)\mathrm{d}\xi \ . \tag{44}$$

We assume that the flow rate is in the following form:

$$q(z,t) = \frac{1}{2}\left\{Q_1 \mathrm{e}^{i(t-t_0)} + Q_2(z)\mathrm{e}^{i(t+\beta(z))} + \bar{Q}_1 \mathrm{e}^{-i(t-t_0)} + \bar{Q}_2(z)\mathrm{e}^{-i(t+\beta(z))}\right\} \ , \tag{45}$$

where Q_1 = const is the contribution to the flow rate due to the catheter movement and $Q_2(z)$ is the amplitude of the flow rate in the absence of catheter oscillations. The phase-difference angle β can be thought of as an indicator of the impedance to flow. Equation (44) along with Eq. (41) gives

$$\begin{aligned} f(0) = \frac{2i}{(1-k^2)}\Bigg\{&\frac{\tilde{a}_{11}}{\alpha_{11}}\left[c_1(0)(I_1(\alpha_{11}) - kI_1(\alpha_{11}k)) + c_2(0)(K_1(\alpha_{11}) - kK_1(\alpha_{11}k))\right] \\ &+ \frac{\tilde{a}_{12}}{\alpha_{12}}\left[d_1(0)(I_1(\alpha_{12}) - kI_1(\alpha_{12}k)) + d_2(0)(K_1(\alpha_{12}) - kK_1(\alpha_{12}k))\right]\Bigg\} \\ &- \frac{2i}{(1-k^2)}\left[\mathrm{e}^{i\beta(0)}Q_2(0) + \mathrm{e}^{-i\,t_0}Q_1\right] \ . \end{aligned}$$

Also,

$$B(0) = -iU_{11}(1,0) \ ,$$

which gives

$$\begin{aligned} f^{(1)}(0) = \frac{2i}{(1-k^2)}\Bigg\{&\frac{\tilde{a}_{11}}{\alpha_{11}}\left[c_1^{(1)}(0)(I_1(\alpha_{11}) - kI_1(\alpha_{11}k)) + c_2^{(1)}(0)(K_1(\alpha_{11}) - kK_1(\alpha_{11}k))\right] \\ &+ \frac{\tilde{a}_{12}}{\alpha_{12}}\left[d_1^{(1)}(0)(I_1(\alpha_{12}) - kI_1(\alpha_{12}k)) + d_2^{(1)}(0)(K_1(\alpha_{12}) - kK_1(\alpha_{12}k))\right]\Bigg\} \\ &- \frac{2B(0)}{(1-k^2)} \ . \end{aligned}$$

Thus $f(z)$ is completely known, if we know B, Q_2 and β at $z = 0$. It may be noted that if $w_c = 0$ then $Q_1 = 0$. For nonzero values of w_c, the contribution of the catheter movement to the flow rate is estimated by finding the difference between the flow rates which are calculated for $w_c = 0$ and $w_c \neq 0$.

3.2
Solution for the $O(\epsilon^2)$ case

Our main purpose of the study is to analyze the steady-streaming velocity components w_{20}, u_{20} and the microrotation component g_{20}, due to the oscillatory fluid flow, as given by Eqs. (31)–(36).

Thus, solving for $w_{20}(\xi, z)$ and $g_{20}(\xi, z)$, we get

$$w_{20}(\xi,z) = \frac{\alpha^2\xi^2}{2(2+\mu_1)}\frac{\mathrm{d}p_{20}}{\mathrm{d}z} + \frac{2\alpha^2 H_1(\xi,z)}{(2+\mu_1)} + \log(\xi)c_3(z) + c_4(z) - 2N^2\int^{\xi} g_{20}(\xi,z)\mathrm{d}\xi \tag{46}$$

and

$$\begin{aligned} g_{20}(\xi,z) = {}& d_3(z)I_1(\alpha_{13}\xi) + d_4(z)K_1(\alpha_{13}\xi) \\ &+ K_1(\alpha_{13}\xi)V_{21}(\xi,z) + I_1(\alpha_{13}\xi)V_{22}(\xi,z) - \frac{\alpha^2\xi}{4}\frac{\partial p_{20}}{\partial z} \\ &+ \frac{a^2\alpha^2}{2+\mu_1}\left[K_1(\alpha_{13}\xi)V_{11}(\xi,z) + I_1(\alpha_{13}\xi)V_{12}(\xi,z)\right] - \frac{c_3(z)}{2(1-N^2)\xi} \ , \end{aligned} \tag{47}$$

where,

$$H_1(\xi,z)=\int^{\xi}\frac{1}{\xi}\left(\int^{\xi}\xi G_1^*\mathrm{d}\xi\right)\mathrm{d}\xi,\quad \alpha_{13}^2=a^2(1-N^2), H_2(\xi,z)=\int^{\xi}\xi G_1^*(\xi,z)\mathrm{d}\xi\ ,$$

$$V_{11}(\xi,z)=-\int^{\xi} I_1(\alpha_{13}\xi)H_2(\xi,z)\mathrm{d}\xi,\quad V_{12}(\xi,z)=\int^{\xi} K_1(\alpha_{13}\xi)H_2(\xi,z)\mathrm{d}\xi\ ,$$

$$V_{21}(\xi,z)=-\int^{\xi}\xi I_1(\alpha_{13}\xi)G_3^*(\xi,z)\mathrm{d}\xi,\quad V_{22}(\xi,z)=\int^{\xi}\xi K_1(\alpha_{13}\xi)G_3^*(\xi,z)\mathrm{d}\xi\ .$$

while $c_3(z)$, $c_4(z)$, $d_3(z)$ and $d_4(z)$ are unknown functions of z to be determined.

The continuity equation corresponding to the case $O(\epsilon^2)$ and the boundary condition at $\xi=k$ for u_{20} give

$$\xi u_{20}=\int_k^{\xi}\xi G_2^*\mathrm{d}\xi-\int_k^{\xi}\xi\frac{\partial w_{20}}{\partial z}\mathrm{d}\xi\ . \tag{48}$$

Now, $u_{20}=0$ at $\xi=1$ gives the following differential equation:

$$\frac{\mathrm{d}p_{20}}{\mathrm{d}z}T_4=\int_0^{z}\left(\int_k^{1}\xi G_2^*\mathrm{d}\xi\right)\mathrm{d}z-d_3(z)T_1-d_4(z)T_2-c_3(z)T_3-c_4(z)T$$
$$-\int_0^{z}\left(\int_k^{1}\xi\frac{\partial F}{\partial z}\mathrm{d}\xi\right)\mathrm{d}z+D_2\ , \tag{49}$$

where

$$T_1=\int_k^{1}\xi b_1\mathrm{d}\xi,\quad T_2=\int_k^{1}\xi b_2\mathrm{d}\xi,\quad T_3=\int_k^{1}\xi b_3\mathrm{d}\xi,\quad T_4=\int_k^{1}\xi b_4\mathrm{d}\xi\quad\text{and}\quad T=\frac{k^2-1}{2}\ ,$$

while D_2 is determined by using the condition

$$\frac{\mathrm{d}p_{20}(0)}{\mathrm{d}z}=0$$

due to the assumption that zero mean flow rate is at $z=0$. This gives

$$D_2=d_3(0)T_1+d_4(0)T_2+c_3(0)T_3+c_4(0)T\ . \tag{50}$$

Boundary conditions (35) and (36) are used to obtain a linear system of equations in $c_3(z)$, $c_4(z)$, $d_3(z)$, $d_4(z)$ and dp_{20}/dz. We solve this system along with Eq. (49) numerically, for each axial location z $(0\le z\le 2\pi)$ and get the solution for $w_{20}(\xi,z)$, $u_{20}(\xi,z)$ and $g_{20}(\xi,z)$, where $k\le\xi\le 1$.

This completes our solution procedure which is valid up to the order of ϵ^2 for the calculation of the time-averaged pressure gradient and velocity components. However, it may be noted that we need $c_1(z)$, $c_2(z)$, $d_1(z)$, $d_2(z)$ and their derivatives for evaluating $f(z)$.

This is being done numerically. To start with, initial values of f are assumed at each axial location z. In our calculation, we have specified $f=1$, $\forall z\in[0,2\pi]$. Functions $c_1(z)$, $c_2(z)$, $d_1(z)$, and $d_2(z)$ are calculated through an iterative process. The tolerance value for the convergence is fixed as 10^{-5}. Finally, the microrotation and velocity components for the $O(\epsilon)$ case are

calculated from Eqs. (40), (41) and (42). Using these values, flow variables for the order of ϵ^2 are obtained numerically. Further, the axial velocity values are differentiated numerically for getting the wall shear stress. It may be mentioned that the calculations involving Bessel functions are made using polynomial approximation expressions as given in [14].

4
Results and discussion

We present were the results based on the above steady-streaming analysis. It may be noted that, apart from the usual dimensionless parameters α (Womersley parameter), β (phase difference between flow-rate and pressure gradient) and k (catheter size), which describe the newtonian flow in a catheterized artery, [6], the steady-streaming analysis in this study also depends upon μ_1 and M. In the following, we discuss the effects of these parameters on the three important outcomes of the analysis, namely, (i) the mean velocity distribution, (ii) the mean pressure gradient, and (iii) the mean wall shear stress.

In all these cases, we have fixed the amplitude of the flow rate at $z = 0$ as $Q_2(0) = 0.5$ and the amplitude of the wall variation at $z = 0$ as $B(0) = 0.05$. These amplitude values correspond to the flow rate and the wall motion described in the $O(\epsilon)$ case, on which steady streaming depends. The maximum amplitude of the catheter oscillation, is $w_c = 0.2$, and the phase lead t_0 of the catheter over the flow is taken zero, due to the fact that t_0 does not have considerable influence on the pressure gradient, [6].

It may be recalled that μ_1 and M characterize the coefficient of vortex viscosity κ and the coefficient of gyroviscosity γ of the micropolar fluids respectively. An increase in κ is reflected as an increase in the parameter μ_1, while an increase in γ results in decreasing values of M. It may be mentioned here that in the context of blood flow studies the viscosity ratio μ_1 represents a polar effect which occurs between blood corpuscles and fluid, [10]. The microstructure size effect parameter M means the ratio of corpuscle to the radius of the annular region. Also, it may be noted that the expression for $w_{20}(\xi, z)$ reduces to the newtonian case as $\mu_1 \to 0$ and $M \to \infty$. In our discussion, the values of the micropolar fluid parameters are taken as $\mu_1 = 0.1, 1.0$ and $M = 1.0, 10.0$.

4.1
Mean velocity distribution

The mean velocity distribution can be calculated using $w_{20}(\xi, z)$ given in Eq. (46). The effect of micropolar parameters on the velocity profile across the annular region ($k \leq \xi \leq 1.0$) is seen by fixing the axial location $z = \pi$ for various values of Womersley parameter α and phase difference β between the flow rate and the pressure gradient. They are shown in Fig. 2 for $k = 0.3$ and $\beta = \pi/3$ and in Fig. 3 for $k = 0.3$ and $\alpha = 0.5$, respectively.

Figure 2 shows that the mean velocity distribution has a parabolic profile similar to the annular flow in a rigid tube. As α increases, the effect of elastic tube wall on the flow brings mild kinks in the neighbourhood of boundary walls. This shows an increased interaction of wall and the oscillatory flow. In the core of annular region, maximum value of mean velocity has a mixed trend as α increases. Higher values of α imply that either the newtonian viscous effect becomes negligible or frequency of flow oscillation is more dominant. Thus the mean velocity profile reacts to the oscillatory nature of flow and the magnitude of mean velocity becomes small. The

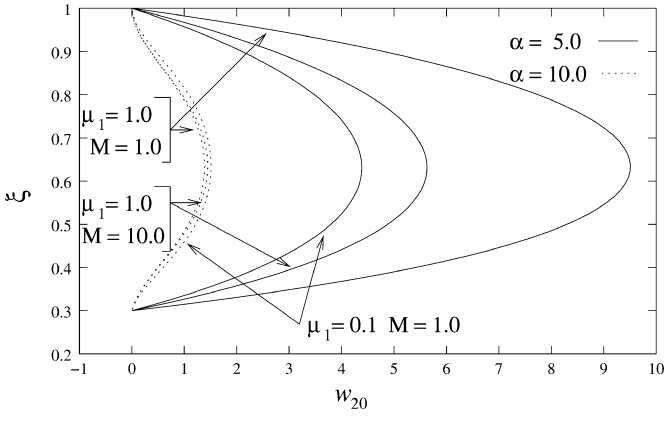

Fig. 2. Distribution of w_{20} ($k = 0.3$, $\beta = \frac{\pi}{3}$, $w_c = 0.2$, z is fixed at π)

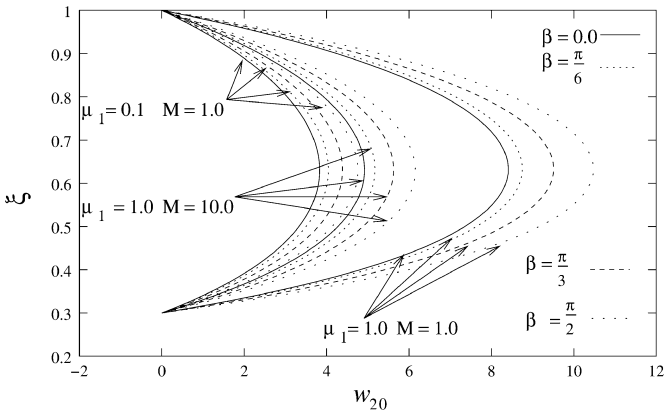

Fig. 3. Distribution of w_{20} ($k = 0.3$, $\alpha = 5.0$, $w_c = 0.2$, z is fixed at π)

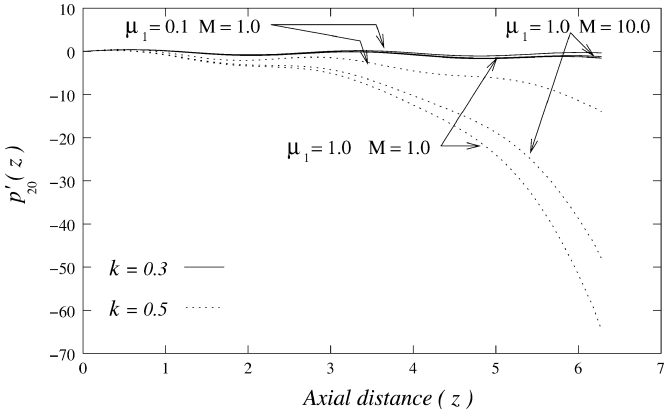

Fig. 4. Distribution of p_{20} ($\alpha = 10.0$, $\beta = \frac{\pi}{3}$, $w_c = 0.2$)

result is similar to the study [6]. An increase in the viscosity coefficient corresponding to micropolar fluid $\mu_1 = 0.1$ to $\mu_1 = 1.0$ implies an increase in mean velocity profile. This indicates the effect of enhanced viscous effect due to viscosity coefficient of micropolar fluid κ. There is no significant change in the mean velocity profile for higher values of α, when $\mu_1 = 1.0$. The influence of microstructure on mean flow is observed through parameter M. An increase in M clearly implies a decrease in mean velocity values for $\mu_1 = 1.0$.

The effect of the phase difference angle β on the velocity profile is shown in Fig. 3. Varying β from 0 to $\pi/2$, we see an increase in the mean velocity and it is enhanced for large values of μ_1. This indicates the importance of considering the phase difference and the micropolar viscosity coefficient κ in our study. It is observed that the parameter M does not significantly influence w_{20} for small values of μ_1 but it does so for large values of μ_1. It is to be noted that mean velocity w_{20} is a correction to the velocity component w, up to order of ϵ^2 calculation, due to steady-streaming.

4.2
Mean pressure gradient

We now discuss pressure gredient dp_{20}/dz wich is the correction to dp/dz. Let us denote $dp_{20}/dz = p'_{20}$. One of the basic interest in this investigation is to understand the time-mean pressure gradient p'_{20}, a characteristic of steady streaming in a distensible tube. It is a correction to the pressure gradient calculated from the theories which neglect convective acceleration effect. Figures 4 to 6 show the mean pressure gradient values across the axial direction z.

Figure 4 displays the effect of the presence of catheter on p'_{20}, where z ranges from zero to 2π, $\alpha = 10.0$ and $\beta = \pi/3$. The catheter radius k takes values 0.3 and 0.5. The oscillatory nature of mean pressure gradient is observed. As expected, an increase in k produces higher mean pressure gradient since flow rate amplitude is fixed at $z = 0$. This increase in p'_{20} can bring more resistance to flow. Further, the mean pressure gradient is increased as a result of an increase in the viscosity ratio μ_1. This is because the viscosity coefficient κ for micropolar fluid

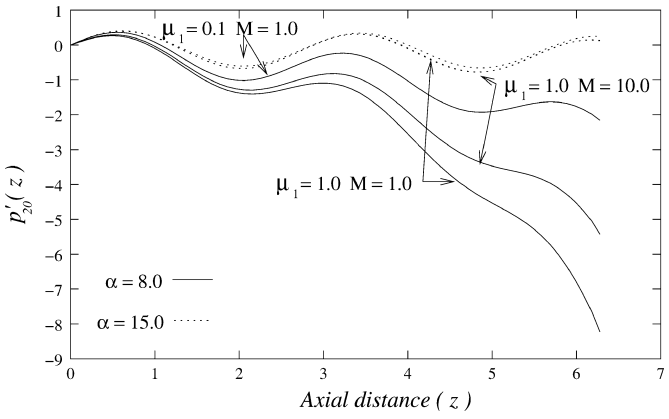

Fig. 5. Distribution of p_{20} ($k = 0.3$, $\beta = \frac{\pi}{3}$, $w_c = 0.2$)

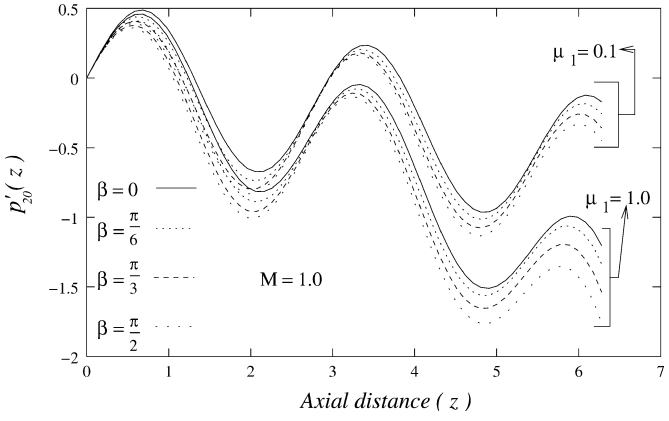

Fig. 6. Distribution of p_{20} ($k = 0.3$, $\alpha = 10.0$, $w_c = 0.2$)

contributes to higher resistance to the mean flow. An increase in the other micropolar parameter M reduces this effect.

Figure 5 depicts the influence of parameter α on p'_{20}. Here, we have fixed $k = 0.3$ and $\beta = \pi/3$. As α increases the magnitude of p'_{20} increases. This can be interpreted as an increase in interaction of the wall and the unsteady nature of flow which induces higher mean pressure gradient. Increasing μ_1 promotes change in p'_{20}, and increasing M reduces that effect.

Figure 6 shows the effect of the phase angle β on p'_{20}. It may be seen that the oscillatory nature of the pressure gradient is preserved and there is a change in p'_{20}, enhanced by varying μ_1. Mean pressure gradient decreases when the size of the microstructure reduces. These results imply the importance of micromotions of micropolar fluid particles in the flow, particularly in the presence of wave reflection β.

4.3
Mean wall shear stress

We define the dimensionless mean wall shear stress for micropolar fluid flow from the order of ϵ^2 calculation as

$$s_{20} = \frac{\partial w_{20}}{\partial \xi}\bigg|_{\xi=1} .$$

Figures 7 and 8 illustrate the nature of mean wall shear stress along the axial direction. In all considered cases, a wavelike pattern of the mean wall shear stress is observed, due to the interaction of the fluctuating flow with the elastic wall. Influence of micropolar parameters on s_{20} is noted for different values of catheter radius k Fig. 7. An increase in k shows an increase in the absolute value of the mean wall shear stress. This is because the reduction in the annular gap increases the wall shear stress. Further, increasing micropolar viscosity coefficient brings out significant change in the mean shear stress. Thus, the polar character of micropolar fluid

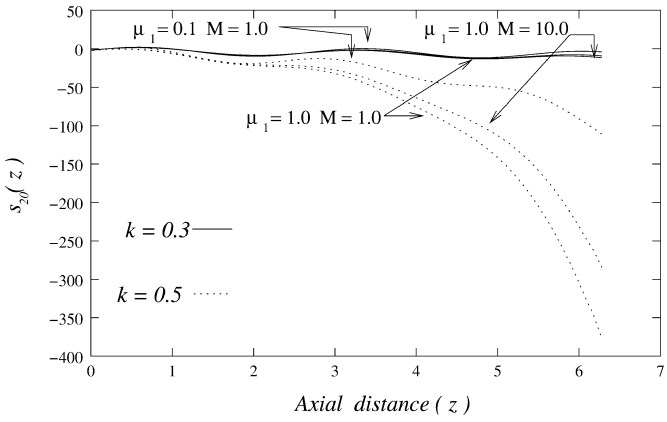

Fig. 7. Distribution of s_{20} ($\alpha = 10.0$, $\beta = \frac{\pi}{3}$, $w_c = 0.2$)

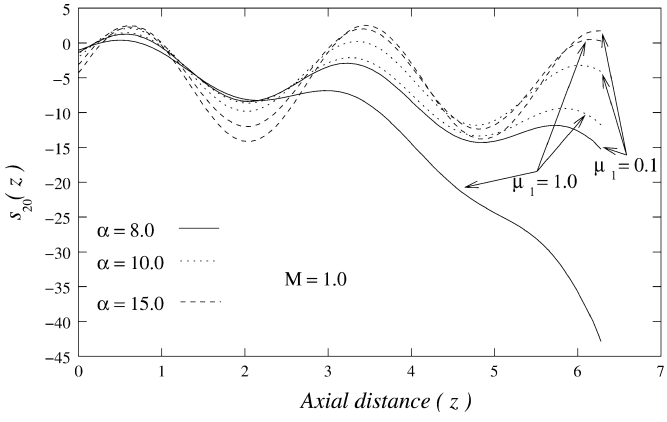

Fig. 8. Distribution of s_{20} ($k = 0.3$, $\beta = \frac{\pi}{3}$, $w_c = 0.2$)

enhances the mean wall shear stress. A decrease in the size of the microstructure relatively reduces the effect of μ_1, especially at $\mu_1 = 1.0$.

The combined influence of α and the micropolar fluid parameters on s_{20} can be seen in Fig. 8. Here, we fix $k = 0.3$ and $\beta = \pi/3$. As α increases, the unsteady nature of the flow increases, and thus the amplitude of the wavelike behaviour of s_{20}.

5
Conclusion

The present paper considers the micropolar nature of a blood flow in a catheterized artery. The steady-streaming phenomenon yields nonzero mean pressure gradient along the axial direction. The influence of the elastic wall on the mean velocity profile is shows in the presence of polarity. Mean wall shear stress and mean pressure gradient show wavelike patterns along the axial direction due to oscillatory flow conditions. The results obtained for various values of the Womersley parameter and the catheter size show a strong increase in the mean quantities with an increase of the magnitude of μ_1. However, the analysis also shows that M has little influence on these results.

References

1. **Kanai, H.; Lizuka, M.; Sakamotos, K.:** One of the problems in the measurement of blood pressure by catheterization : wave reflection at the tip of catheter. Med Biol Eng 28 (1970) 483–496
2. **Macdonald, D.A.:** Pulsatile flow in a catheterized artery. J Biomech 9 (1986) 239–249
3. **Back, L.H.:** Estimated mean flow resistance increase during coronary artery catheterization. J Biomech 27 (1994) 169–175
4. **Wang, D.M.; Tarbell, J.M.:** Nonlinear analysis of flow in an elastic tube(artery): steady streaming effects. J Fluid Mech 239 (1992) 341–358
5. **Wang, D.M.; Tarbell, J.M.:** Nonlinear analysis of oscillatory flow, with a nonzero mean, in an elastic tube (artery). Trans. ASME J Biomech Eng 117 (1995) 127–135
6. **Sarkar, A.; Jayaraman, G.:** Nonlinear analysis of oscillatory flow in the annulus of an elastic tube: application to catheterized artery. Phy Fluids 13 (2001) 2901–2911
7. **Eringen, A.C.:** Theory of micropolar fluids. J Math Mech 16 (1966) 1–18

8. **Ariman, T.; Turk, M.A.; Sylvester, N.D.:** On the steady and pulsatile flow of blood. J Appl Mech 41 (1974) 1–7
9. **Lukaszewicz, G.:** Micropolar Fluids: Theory and Applications. Birkhäuser Boston, 1999
10. **Sawada, T.; Tanahashi, T.; Ando, T.:** Oscillatory flow of a micropolar fluid as a model for blood flow. KEIO Science and Technology Reports 35 (1982) 105–121
11. **Mizukami, Akiras:** Nonsteady shear flow of micropolar fluids. Int J Eng Sci 19 (1981) 75–82
12. **Kline, K.A.; Allen, S.J.:** Nonsteady flows of fluids with microstructure. Phys. Fluids 13 (1970) 263–270
13. **Prakash, J.; Sinha, P.:** Squeeze film theory for micropolar fluids. Trans. ASME J Lubrication Tech 98 (1976) 139–144
14. **Abramowitz, M.; Stegun, I.A.:** Handbook of Mathematical Functions. National Bureau of Standards, Applied Mathematical Series 55 (1964) p. 378